Concentration dependent structural behavior of Gd_2O_3 nanocrystallites dispersed in silica matrix

RACHNA, NIDHI, INDU YADAV, D.S. AHLAWAT, P. AGHAMKAR
Department of Physics, Materials Science Lab, Ch. Devi Lal University, Sirsa-125055, Haryana, India

Nanocrystalites of Gd_2O_3 have been successfully synthesized by sol-gel process using hydrochloric acid as a catalyst. $Gd(NO_3)_3.6H_2O$ and TEOS were used as precursors and obtained powdered form of Gd_2O_3:SiO_2 powder. The powdered samples having 2.2 and 3.4 mol % Gd_2O_3 were annealed at 500°C and 900°C temperature for 6h and characterized by X-ray diffraction (XRD), Fourier transforms infrared spectroscopy (FTIR), Scanning electron microscopy (SEM) and Transmission electron microscopy (TEM). The effects of sintering temperature and concentration of gadolinium oxide on the phase evolution of the prepared sample have been discussed in detail. The powdered samples having 2.2 mol % Gd_2O_3 do not show any crystalline structure probably due to low concentration of gadolinium oxide. The pure cubic phase of gadolinium oxide was completely developed in annealed sample having 3.4 mol % Gd_2O_3. The average nanocrystallite size was calculated ~ 21 nm using well known Debye-Scherrer's equation.

(Received October 20, 2014; accepted May 7, 2015)

Keywords: Gadolinium oxide, Silica, FTIR, SEM and TEM

1. Introduction

Rare earth oxides have been extensively investigated due to their fascinating properties such as enhanced luminescence efficiency; lower lasing threshold, high-performance luminescent devices, drug-carrying vehicle, contrast agent in Magnetic Resonance Imaging (MRI), up-conversion materials, catalysts, and time-resolved fluorescence (TRF) labels for biological detection etc [1-2]. Due to these merits, they have various technologically important applications, like in luminescent lighting, plasma display panels, flat panel displays, high definition televisions, in biomedical applications, as sensors, as IR windows, nanoheaters, latent fingerprint detection, etc [3-5]. Among rare earth oxides Gadolinium oxide (Gd_2O_3) is an Ln_2O_3-type oxide has been extensively studied due to its optoelectronic, data storage, sensors, scintillator, solid electrolytes and display applications [6-7]. The rare earth oxides are very expensive and this has limited their use in a number of technical applications. Combining the promising properties of Gd_2O_3 with nanoparticles in the form of powder of inert host is important for the fabrication of the cost efficient nanocomposites. Silica forms an interesting class of matrices for the deposition of metals, oxides, and functional polymers. Various groups have employed some wet chemical methods to coat silica spheres with nanoparticles of noble metals, rare earth oxides, and transition metal oxides [8-9].

Sol–gel technology appears a possible tool in order to produce composite materials constituted by rare earth oxide embedded into an inert host. This may provide a convenient way for tailoring rare earth-oxide nanoparticles of nearly uniform sizes and for facilitating homogeneous dispersion in the silica matrix [10]. D.D. Martino et al. [11] have tried to investigate the effect of concentration on the structural properties of gadolinium in sol-gel silica. They have used rapid thermal treatment (RTT~ 1500-1800°C) and emphasized that gadolinium concentration higher than 3 mol % induce remarkable modification of the IR spectra. But they have not studied the effect of sintering temperature on the prepared samples. S. Mukherjee et al. [12] have successfully synthesized nanocrystalline Gd_2O_3 particles (0.2 mol %) in silica glass matrices by a sol–gel method at 700°C and above. Here we can say that nanocrystalline Gd_2O_3 developed at much higher temperature probably due to the low concentration of the dopant.

In the backdrop of these findings, our goal is to investigate the incorporation of gadolinium oxide in silica matrix and to study the effect of concentration and temperature on the prepared powdered samples. In the present instance, the percentage of gadolinium oxide is taken as 2.2 and 3.4 mol % in Gd_2O_3:SiO_2 powdered samples and the morphology of nanocrystallites thus obtained is ascertained from XRD, FTIR, SEM and TEM experimental techniques.

2. Experimental

2.1 Sample preparation

Using sol-gel technique hydrous gadolinium nitrate and hydrous silicon oxide were mixed at room temperature. For this purpose high purity reagents: Tetraethoxysilane (Aldrich 99.99%), ethanol (Merck 99.9%) and double distilled water were mixed in the presence of hydrochloric acid as catalyst. The detailed description of the synthesis route was reported elsewhere [13] where a specific molar ratio of the precursors was taken to prepare Gd_2O_3:SiO_2 nanocomposites. The dried

sample is named as-prepared and designated as (a). Furthermore, the dried samples were annealed in a programmable furnace at different temperatures to study the effect of heat treatment on phase evolution of Gd_2O_3:SiO_2 powdered samples. In forthcoming subsections annealed samples are designated as: (b) for 500°C and (c) for 900°C.

2.2 Characterizations

As-prepared and sintered samples were characterized by an X'pert Pro X-Ray Diffractometer with Cu-$k_{\alpha 1}$ radiation in the range of 5°-80° in steps of 0.017° (40 mA, 45 KV) and further conformed by Hitachi 4500 Transmission electron micrograph (TEM). The surface morphology has been studies by the help of JEOL-JSM-6100 scanning electron microscope (SEM). Infrared spectra (FTIR) of as-prepared and sintered samples were collected by Perkin-Elmer Spectrum 400 spectrophotometer in 4000 - 450 cm^{-1} range to obtained information about phase composition and bonding in the samples.

3. Results and discussion

3.1. X-Ray Diffraction (XRD)

The X-ray diffraction patterns of as prepared Gd_2O_3:SiO_2 powder having 2.2 mol % Gd_2O_3 and annealed at 500°C and 900°C are shown in the Fig. 1 (i). It can be seen that the as prepared sample shows a loosen structure due to the amorphous nature of the precursors. When the sample was annealed at 500°C, no significant change is observed in the diffractogram (b). With the increase of sintering temperature up to 900°C, a slightly broad hump is appeared in the XRD pattern of sample (c) at 2θ ~ 28.5°. Therefore, one can say that at such a low concentration of Gd_2O_3 (2.2 wt %) crystalline phase is hardly appeared even at higher temperature ~ 900°C.

In Fig. 1 (ii) has a sharp and intense diffraction line at 2θ ~ 15.85° along with some weaker peaks at 2θ ~ 14.44°, 16.74°, 17.53°, 18.73°, 20.38°, 29.59°, 32.00°, 34.64° and 36.25°. All these peaks assigned to the intermediate phases of Gadolinium nitrate hydrate $Gd(N\text{-}OH)_3$ product. A small reflection centered at about 2θ ~ 21.38° may be assigned to crystoballite phase of silica [JCPDS Card no. 39-1425] in the differactogram [14]. The XRD pattern of the sample sintered at 500°C (b), shows that a new broad peak at 2θ ~ 28.66° is appeared may be due to applied thermal treatment. One may also notice that all the peaks present in the as-prepared sample are completely disappeared, which indicates the decomposition of gadolinium nitrate hydrate phase of the precursor and the development of initial crystalline structure of cubic Gd_2O_3.

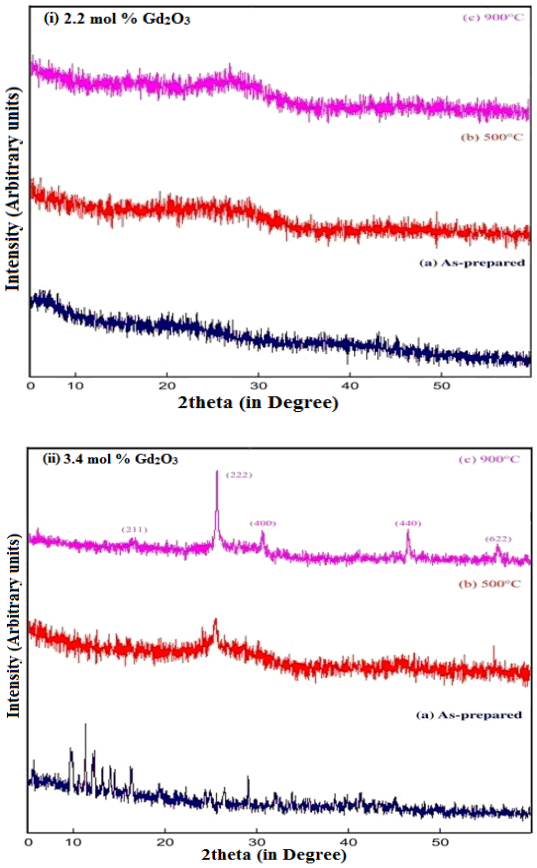

Fig. 1. XRD patterns of Gd_2O_3:SiO_2 powdered sample having (i) 2.2 mol % Gd_2O_3 and (ii) 3.4 mol % Gd_2O_3.

Further, temperature was raised to 900°C for examine the effect of thermally stored energy on structural behavior of Gd_2O_3:SiO_2. At this temperature, the appeared diffraction peaks are assigned to cubic Gd_2O_3 having lattice constant a = 10.80 Å and space group Ia3 (206) [JCPDS card no. 43-1014] [15]. Check cell program was used to obtain the lattice constant, symmetry of powdered samples and miller indices which were found to be (222), (400), (440), and (622) corresponding to diffraction peaks appeared at 2θ ~ 28.75°, 33.31°, 47.70° and 56.57°. Here it is worth mentioning that XRD pattern of the Gd_2O_3:SiO_2 powder sample mainly displayed the peaks of cubic Gd_2O_3 crystalline phase, because the diffraction intensity of silica matrix was too weak so that it shielded by the diffraction peaks of the cubic Gd_2O_3. Moreover, there is no trace of Gadolinium silicates which manifest that the structure of cubic Gd_2O_3 remains stable at 900°C temperature. Thus we may except that in higher loaded samples, crystalline phase of cubic Gd_2O_3 developed more frequently even at a low temperature ~500°C. We know that in annealing process dislocations become the main lattice defect, which decreases with increasing temperature. By the knowledge of average ctystalline size, one may also estimate minimum dislocation density ($\rho \approx 1/\langle D \rangle^2$) of that structure [16]. The dislocation density of nanocrystalline Gd_2O_3 was found to be ~ 2.5×10^{15} m^{-2}. From the above results we may conclude that the sintering temperature and typical concentration of dopant (more than 2 mol %) is

responsible for the development of initial crystalline phase of cubic Gd_2O_3 in Gd_2O_3:SiO_2 powder.

3.1.1. Williamson-Hall (W-H) analysis

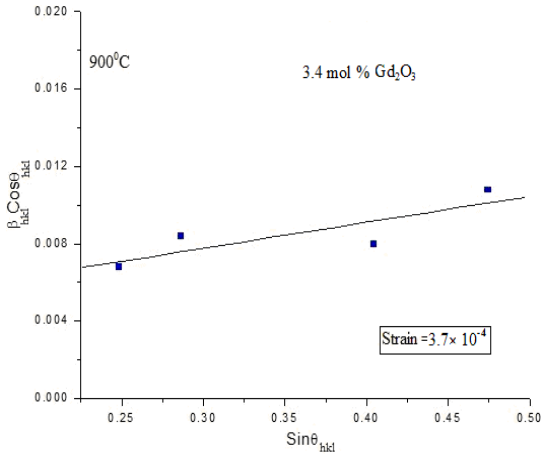

Fig. 2. W-H plot for Gd_2O_3:SiO_2 powder sample having 3.4 mol % Gd_2O_3 at 900°C.

The strain and crystallite size produces peak broadening in the diffraction pattern. The crystallite size and the strain effect have to be differentiated in the diffraction pattern. Both effects are independent and can be distinguished by W–H plot. In order to measure lattice strain and crystallite size, we eliminated the instrumental broadening using standard silica sample X-ray powder diffraction data using the equation:

$$\beta_{hkl} = [(\beta_{hkl})^2_{measured} - \beta^2_{(instrumental)}]^{1/2} \quad (1)$$

where β_{hkl} is the full width at half maximum. As-prepared XRD pattern shows asymmetry which may be due to the lattice strain [17]. However, for the sample sintered at 900°C, the lattice strain is reduced. Since the annealed samples are well crystalline and single phase (cubic phase), the crystallite size and the strain can be estimated from W–H method [18].

The W-H equation is:

$$\beta_{hkl}\cos\theta_{hkl} = \frac{k\lambda}{d} + 2\epsilon\sin\theta_{hkl} \quad (2)$$

where K is the shape factor which is 0.9 for uniform small size crystals, λ is the wavelength of X-ray, θ_{hkl} is the Bragg angle, ϵ is the strain and d is a average crystalline size measured in a direction perpendicular to the surface of the specimen. Due to small crystalline size and micro strain present in the material, the XRD peaks broadening can be distinguished from Williamson-Hall (W-H) plot. It is well known that the crystallite size and strain contributions to line broadening are independent of each other. Here, the W-H plot was examined only for annealed (900°C) sample because of its well crystalline nature. The graph is plotted between $\sin\theta_{hkl}$ and $\beta_{hkl}\cos\theta_{hkl}$ as shown in the Fig. 2. The lattice strain was calculated by the slope of straight line and has negligible value ~3.7×10^{-4}. It is noticed that micro-strain reduces gradually with increasing annealing temperature and its influence on broadening XRD peak is negligibly small. Under such considerations (ϵ = 0), Williamson-Hall relation reduces to Debye-Scherer's equation:

$$D = K\lambda/\beta\cos(\theta) \quad (3)$$

where θ is the Bragg angle of diffraction lines, λ is the wavelength of incident X-ray and β is the full width at half maximum (FWHM). The average crystalline size (*D*) of the nanocrystallites was calculated using equation (3) and found to be 12 nm and 21 nm for the samples annealed at 500°C and 900°C, respectively.

3.2 Fourier Transforms Infrared Spectroscopy (FTIR)

FTIR spectra of Gd_2O_3:SiO_2 having 2.2 mol % Gd_2O_3 is shown in the Fig. 3 (i). Using FTIR spectroscopy (4000-450 cm^{-1}) structural changes of the heat treated powdered samples is explained. Water bands observed at ~3400 and 1646 cm^{-1} corresponding to stretching and bending vibrations of H-O-H bond [19-20]. Strong bands observed at 1103, 814, 466, 961 cm^{-1} have been attributed to Si-O-Si (symmetric, asymmetric, bending) and Si-OH absorptions, respectively [21-22]. Sharp peak at 1384 cm^{-1} is assigned to $-NO_3$ group (present due to dissolution of gadolinium in conc. HNO_3 acid) along with small peak at 748 cm^{-1} due to NO_3 asymmetric stretching. Absorption bands at 1333 and 1477 cm^{-1} are attributed to C=O and N-OH symmetric stretching [23]. When the sample was sintered at 500°C, absorption bands of impurities like H_2O and NO_3 become less intense and peak corresponding to Si-OH is almost disappeared. Further, at 900°C, mostly water and nitrate groups are evaporated in FTIR spectra which in turn confirm the densification of the composite. No absorption peak corresponding to Gd-O bond is appeared in sample (c) having low concentration (2.2 mol %) which is well in agreement with our XRD results.

FTIR spectra of Gd_2O_3:SiO_2 powder having 3.4 mol % Gd_2O_3 are shown in the Fig. 3 (ii) with in the spectral range of 4000 – 450 cm^{-1}. A typical FTIR spectrum of sample (a) shows that the entire absorption bands lie much deeper as compared to the lower concentration samples shown in the Fig. 3 (i). In the Fig. 3(ii), region centered at 3490 cm^{-1} is assigned to the stretching vibration of H-O-H and surface silanol group (Si-OH), respectively [19-20]. The absorption bands around 1641 and 1384 cm^{-1} are due to bending of H-OH absorbed at silica surface and symmetric stretching of $-NO_3$ group, respectively [21-23]. The absorption bands around 1100, 814 and 464 cm^{-1} are attributed to symmetric, asymmetric stretching and bending vibrations of the Si-O-Si bond, respectively while a shoulder at 961 cm^{-1} could be assigned to Si-OH silanol group [20-22]. A sharp peak at 1384 cm^{-1} along with small absorption at 708 and 1489 cm^{-1} is assigned to symmetric, asymmetric stretching of $-NO_3$ and C=O groups [23-25].

At 500°C, there is significant decrease in absorption bands around 3418, 1636 and 1384 cm^{-1} due to evaporation of absorbed water and $–NO_3$ gases. Bands at 961 cm^{-1} and 708 cm^{-1} are almost disappeared at this temperature. FTIR spectrum of the sample sintered at 900°C (c) reveals an important result that a strong and intense characteristic peak of Gd-O (Metal-oxygen) was appeared at 566 cm^{-1} which is well in agreement with the literature [26-27] and XRD results of the same sample. Almost impurities are absent in the trace of sample which strengthened the pure cubic crystalline nature of Gd_2O_3. The absorption band at 1384 cm^{-1} confirms that nitrate groups are not burnt and still remains in the sintered sample at 900°C.

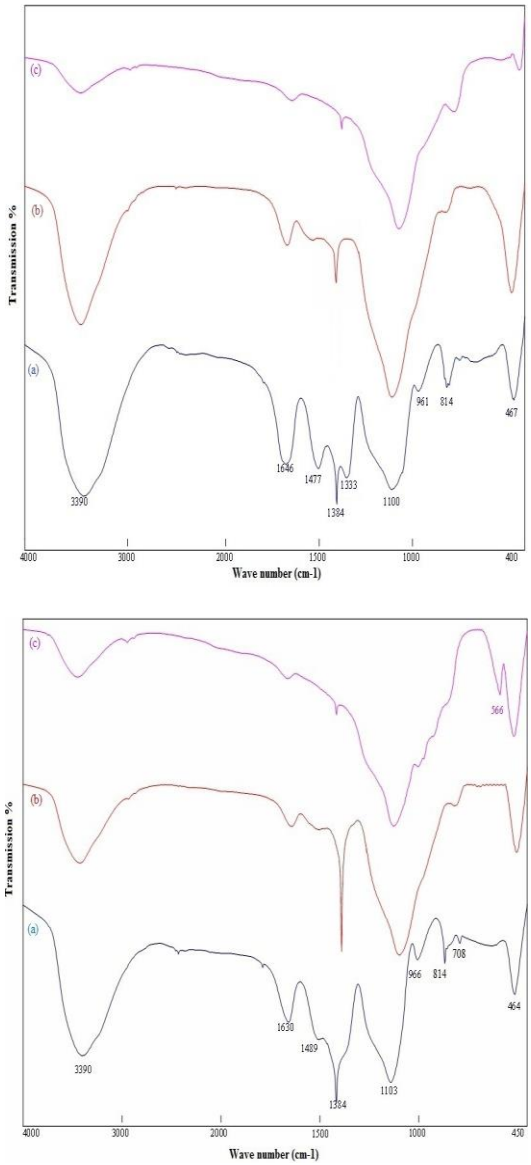

Fig. 3. FTIR spectra of powdered samples having (i) 2.2 mol % Gd_2O_3 and (ii) 3.4 mol % Gd_2O_3 where (a) is as prepared sample (b) at 500°C (c) at 900°C.

3.3 Scanning Electron Microscopy (SEM) Analysis

Fig. 4 shows SEM images of different types of morphologies of composite having 2.2 mol % Gd_2O_3 as viewed under scanning electron microscope. The sample (a) shows humps of irregular shapes which indicate the amorphous nature of the precursors. The sample (b) sintered at 500°C for 6 h shows various types of morphologies including quasi-spherical and rod like. In this image reflection from the surfaces of the grains infers the hygroscopic nature of the precursors as well as persistence of water. Therefore annealing of the prepared sample at this temperature is not effective even for achieving initial crystalline phase of composite. When the calcinations temperature was increased up to 900°C, the SEM image shows much-improved disparity and decrease in contents of water molecules, Si-OH and volatiles. Also, some black patches in the Fig. 4 (c) are replaced by white patches results in densification of the sample due to increased sintering temperature. But the composite is still in amorphous form having size in micrometer range. Thus, in present concentration and thermal treatment, micrograph does not show any development of crystalline phases in Gd_2O_3:SiO_2 powder. However, some changes in morphology observed when the concentration of gadolinium was increased in the sample.

Fig. 5 shows the microstructures of 3.4 mol % Gd_2O_3 doped silica samples. The morphology of as-prepared sample (a) shows effect of increased concentration of gadolinium oxide in the prepared composite. When the sample was sintered at 500°C, the crystalline phase of cubic gadolinium oxide has appeared as white portion of micrograph. Sample (b) consists of small coarse grains with irregular shape and size which are agglomerated somehow. Further, at 900°C in sample (c), mostly white patches were appeared and the structures of patches are similar to the rod shaped and thick lamellar structure.

The crystalline phase of cubic gadolinium oxides is confirmed by the replacement of dark patches by white patches in the micrograph (c). Thus at this temperature and typical concentration, most of the dark patches were replaced by white patches and densification in the structure was considerably enhanced [14]. This result of SEM micrograph is supported by the XRD and FTIR data of the corresponding conditions. A significant change in grain sizes is also observed in (c) and mono disparity of the Gd_2O_3 nanoparticles observed in few nanometers (10-20 nm) which is further confirmed by TEM micrographs.

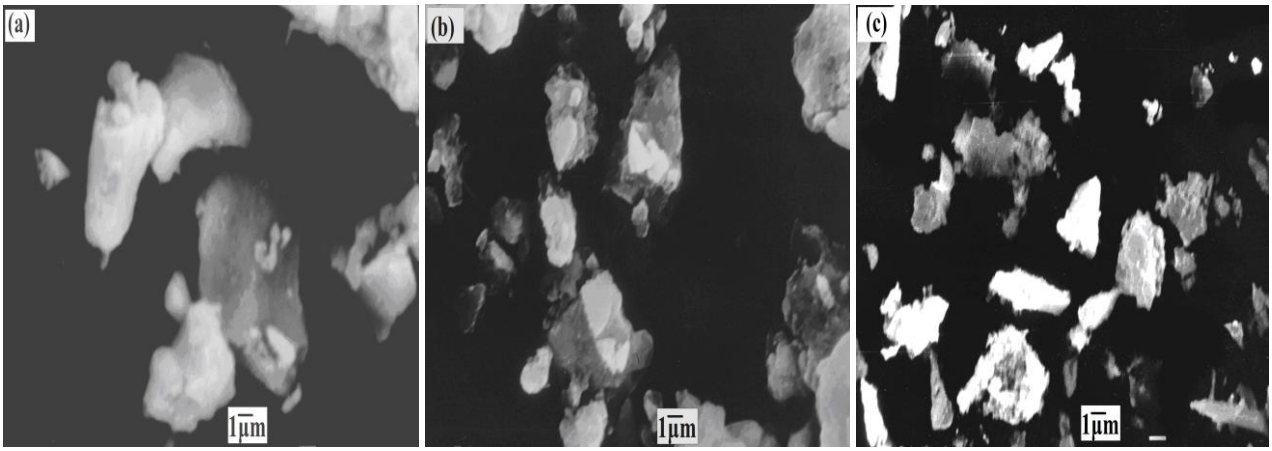

Fig. 4. SEM micrographs of powdered samples having 2.2 mol % Gd_2O_3 (a) as prepared and sintered at (b) 500°C, (c) 900°C.

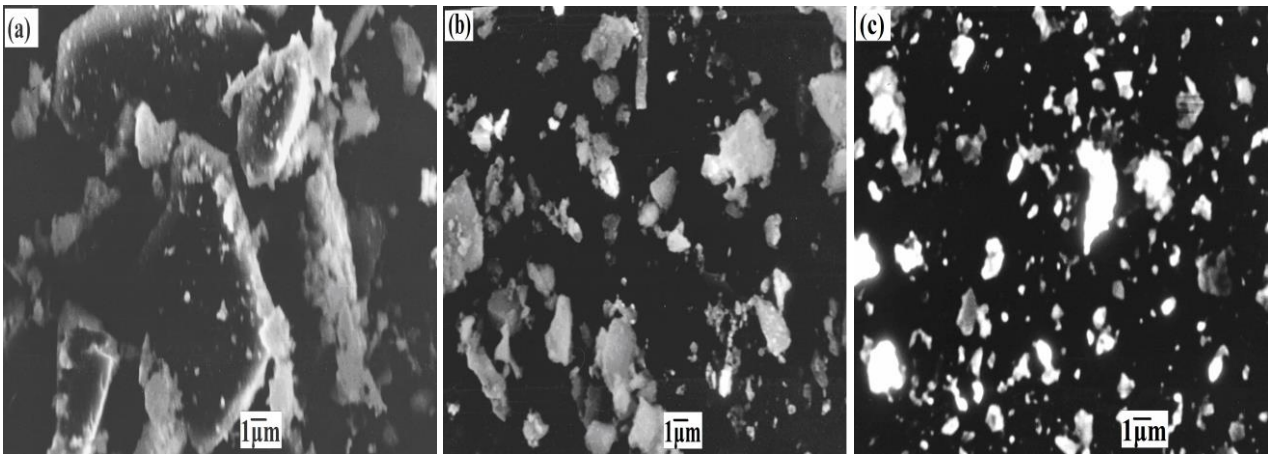

Fig. 5. SEM micrographs of powdered samples having 3.4 mol % Gd_2O_3 (a) as prepared and sintered at (b) 500°C, (c) 900°C.

3.4 Transmission electron Microscopy (TEM) analysis

Fig. 6 represents the transmission electron microscopy of the Gd_2O_3:SiO_2 nanocomposite having different concentration of gadolinium oxide. The TEM images have been observed for the samples sintered at 900°C for both the concentrations.

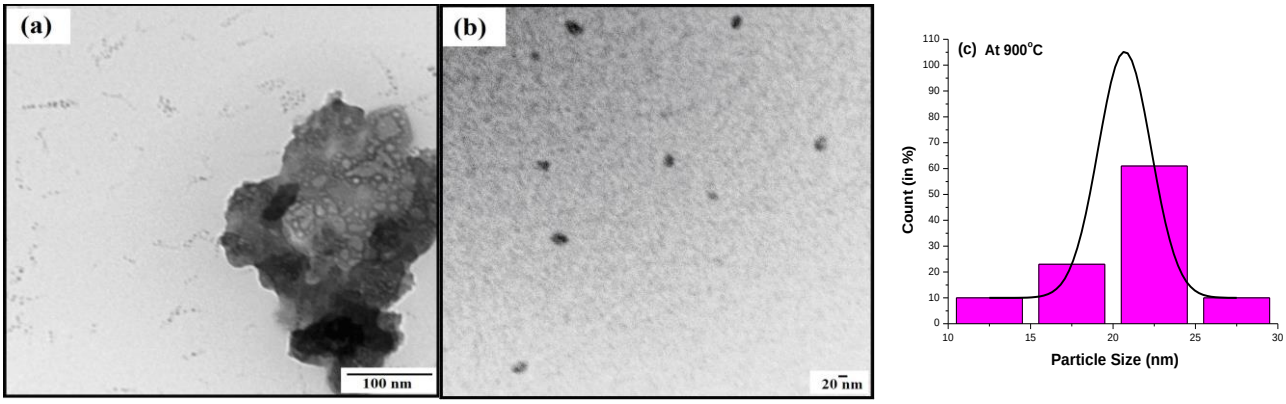

Fig. 6. (a) TEM micrograph of Gd_2O_3:SiO_2 sample having 2.2 mol % Gd_2O_3 (b) Sample having 3.4 mol % Gd_2O_3 sintered at 900°C (c) Particle size distribution.

The micrograph in the Fig 6 (a) show that the sample containing 2.2 mol % of Gd_2O_3 sintered at 900°C for 6h is indicates the water contents in the prepared sample. Sintering of sample may be contributed for agglomeration of Gd_2O_3 in the silica matrix as a result of strong interaction between the nanoparticles and high surface energy as shown in the Fig. 6 (a). In the Fig. 6 (b), the TEM image of prepared sample having 3.4 mol % of Gd_2O_3 is shown which infers that with the rise in concentration, the crytallinity is also improved and spherical shaped gadolinium oxide has been homogenously dispersed in the silica matrix. In the final stage sintering at 900°C, the contents of water molecules, Si-OH and volatiles matter contents has been decreased and the densification of the sample has increased. Most of the particles were found in the order of 22 nm, but there were also some smaller (15 nm) and bigger nanocrystallites (upto 35 nm) as indicated by the particle size distribution shown in the Fig. 6 (c). The measurement infers that the particle size distribution is relatively narrow in the range of 20-25 nm.

4. Conclusions

Using sol-gel process Gd_2O_3:SiO_2 nanocomposites were successfully obtained upon heat treatment in air. Low concentration of gadolinium oxide (2.2 mol %) and sintering at 500°C does not supports the initial crystalline phase of the cubic gadolinium oxide which is further developed at 900°C when concentration was increased up to 3.4 mol %. Sintering temperature in low concentration sample results in aggregation in the nanocomposites is due to solid-state bonds formed between nanoparticles and the gel. The nanocrystalline size for Gd_2O_3:SiO_2 composite was calculated ~22 nm by the help of Debye-Scherer's equation and further confirmed with TEM micrographs. Micro strain value was also calculated using W-H plot and found $\sim 3.7 \times 10^{-4}$. The dislocation density of the same sample was calculated $\sim 2.5 \times 10^{15}$ m^{-2}.

References

[1] S. K. Singh, K. Kumar, S. B. Rai, Mater. Sci. Eng. B **166**, 180 (2010).

[2] V. Bedekar, D. P. Dutta, M. Mohapatra, S. V. Godbole, R. Ghildiyal, K. Tyagi, Nanotechnology **20,** 125707 (2009).

[3] S. K. Singh, A. K. Singh, D. Kumar, O. Prakash, S. B. Rai, Appl. Phys. B: Lasers Opt. **98,** 173 (2010).

[4] M. K. Devaraju, S. Yin, T. Sato, Nanotechnology **20**, 305302 (2009).

[5] J. Gomes, A. M. Pires, O. A. Serra, J. Fluoresc. **16**, 411 (2006).

[6] Z. M. Qi, C. S. Shi, W. W. Zhang, W. P. Zhang, T. D. Hu. Appl. Phys. Lett. **81,** 2857 (2002).

[7] K. Lebbou, P. Perriat, O. Tillement, J. Nanosci. Nanotechnol **5,** 1448 (2005).

[8] V.G Pol., A Gedanken., J.C. Moreno, Chem. Mater. **15,** 1111 (2003).

[9] K.D. Kim, H.J. Bae, H.T. Kim, A **221**, 163 (2003) .

[10] G. Sinha, S. K. Panda, P Mishra., D Ganguli., S. Chaudhuri, J. Phys.: Condens. Matter **19,** 346209-1 (2007).

[11] D.D. Martino, N. Chiodini, M. Fasoli, F. Moretti, A. Vedda, A. Baraldi, E. Buffagni, R. Capelletti, M Mazzera., M. Nikl, G. Angella, C.B. Azzoni, J. Non-Crystalline Solids **354**, 3817 (2008).

[12] S. Mukherjee, P. Dasgupta, P.K. Jana, J. Phys. D: Appl. Phys. **41**, 215004 (2008).

[13] Rachna, P. Aghamkar, Optical Materials **36,** 337 (2013).

[14] S. Duhan, P. Aghamkar, M. Singh, Research Letters in Physics **2008**, 237023 (2008).

[15] Steiner C, Bolliger B Erbudak M, Phys. Rev. B **62**, 10614 (2000).

[16] P. Aghamkar, S. Duhan, M. Singh, N. Kishore, P.K. Sen, J. Sol-Gel Sci Technol **46**, 17 (2008) .

[17] S.T. Tan, B.J. Chen, X.W. Sun, W.J. Fan, H.S. Kwok, X.H. Zhang, S.J. Chua, J. Appl. Phys. **98,** 013505 (2005) .

[18] K. Sun, W.H. Lee, W.M. Risen, J. Non-Cryst. Solids **92**, 145 (1987).

[19] R.F. Bartholomew, B.L. Butler, H.L. Hoover, C.K. Wa, J. Am. Ceram. Soc.**63,** 481 (1980).

[20] L.G. Hwa, S.L. Hwang, L.C. Liu, J. Non-Cryst. Solids, **238**, 193 (1998).

[21] S-Y Chen, C-C Ting, C-H Li, J. Mater. Chem. **12**, 1118 (2002).

[22] L.G. Jacobsohn, M.W. Blair, S.C. Tornga, L.O. Brown, B.L. Bennett, J. Appl. Phys. **104,** 124303 (2008).

[23] Y.K. Kim, H.K. Kim, D. K. Kim, J. Mater. Res. **19,** 2 (2004) .

[24] Z. Xu, J. Yang, Z. Hou, C. Li, C. Zhang, S. Huang, J.M, Lin Materials Research Bulletin **44,** 1850 (2009).

[25] C. Louis, R. Bazzi, M. Flores A., W. Zheng, K. Lebbou, O. Tillement, B. Mercier, C. Dujardin, P. Perriat, Journal of Solid State Chemistry **173,** 335 (2003).

[26] G. Kaur, S.K. Singh, S.B. Rai, J. Appl. Phys. **107,** 073514 (2010).

[27] G. Z. Li, M. Yu, Z. L. Wang, J. Lin, R. S. Wang, J. Fang, J. Nanosci. Nanotechnol. **6**, 1416 (2006) .

*Corresponding author: rachnaahlawat2003@yahoo.com